CHAPTER 61

NONLINEAR WAVE TRANSFORMATION DUE TO A SUBMERGED BREAKWATER

Masahiko Isobe[1], Akira Watanabe[1] and Shogo Yamamoto[2]

Abstract

A nonlinear model of wave transformation due to a submerged breakwater is developed on the basis of the nonlinear mild-slope equations. Numerical computation shows that significant amount of wave energy can be transferred from the fundamental component to higher harmonics by adjusting configuration of the submerged breakwater. In case of oblique incidence, wave direction as well as wave period changes due to the breakwater. These results implies the possibility to control wave period and direction as well as wave height.

1 Introduction

When waves propagate in a region of rapidly changing depth such as over a submerged breakwater, higer harmonic components are generated due to nonlinear effect. Various numerical simulations have been carried out for nonlinear wave transformation due to a submerged breakwater (Ohyama and Nadaoka, 1992, 1994; Tsubota *et al.*, 1994). This implies that submerged breakwaters can change and control characterictics of waves such as wave height, peirod and direction, which can be utilized in coastal engineering. Since floating breakwaters are, in general, effective for controling only short period waves, combination of submerged and floating breakwaters may become an efficient breakwater system. Change of frequency spectrum over an offshore bar is an essential factor in predicting wave field and resultant wave-induced nearshore current. These indicate the importance to study wave transformation due to a submerged breakwater.

Since generation of higher harmonics is a strongly nonlinear phenomenon, it cannot be reproduced by linear or weakly nonlinear wave theories. Isobe (1994) derived a set of nonlinear mild-slope equations which includes full nonlinearity and full dispersion. In the present study, numerical simulations are performed based on the nonlinear mild-slope equations to examine the function of a submerged breakwater to control not only wave height but also wave period and direction.

2 Basic Equations and Boundary Conditions

2.1 Nonlinear mild-slope equation

Fully nonlinear and fully dispersive wave theories have been developed by Nadaoka *et al.* (1994), Nochino (1994) and Isobe (1994) among which the nonlinear mild-slope equations derived by Isobe (1994) is employed in the following numerical simulation.

[1]Dept. of Civil Eng., Univ. of Tokyo, 7-3-1 Hongo, Bunkyo-ku, Tokyo 113, Japan.
[2]Penta-Ocean Construction Inst. of Tech., Nishinasuno-machi, Nasu-gun, Tochigi 329-27, Japan.

In deriving the nonlinear mild-slope equations, the velocity potential, ϕ, is expanded into a series in terms of a set of vertical distribution functions, Z_α, which are given a priori:

$$\phi(\mathbf{x}, z, t) = \sum_{\alpha=1}^{N} Z_\alpha(z; h(\mathbf{x}))\, f_\alpha(\mathbf{x}, t) \equiv Z_\alpha\, f_\alpha \tag{1}$$

where h is the water depth, $\mathbf{x} = (x, y)$ the horizontal coordinates, z the vertical coordinate, t the time, and N the total number of terms.

By substituting the above expression into the Lagrangian defined by Luke (1967), applying the variational principle, and neglecting terms of the second order in bottom slope, the following equations can be obtained:

$$g\eta + Z_\beta^\eta \frac{\partial f_\beta}{\partial t} + \frac{1}{2} Z_\gamma^\eta Z_\beta^\eta \nabla f_\gamma \nabla f_\beta + \frac{1}{2}\frac{\partial Z_\gamma^\eta}{\partial z}\frac{\partial Z_\beta^\eta}{\partial z} f_\gamma f_\beta + \frac{\partial Z_\gamma^\eta}{\partial h} Z_\beta^\eta f_\gamma \nabla f_\beta \nabla h = 0 \tag{2}$$

$$Z_\alpha^\eta \frac{\partial \eta}{\partial t} + \nabla(A_{\alpha\beta}\nabla f_\beta) - B_{\alpha\beta} f_\beta + (C_{\beta\alpha} - C_{\alpha\beta})\nabla f_\beta \nabla h + \frac{\partial Z_\beta^\eta}{\partial h} Z_\alpha^\eta f_\beta \nabla\eta \nabla h = 0 \tag{3}$$

where η is the water surface elevation, g the gravitational acceleration and

$$Z_\alpha^\eta = Z_\alpha|_{z=\eta} \tag{4}$$

$$A_{\alpha\beta} = \int_{-h}^{\eta} Z_\alpha Z_\beta\, dz \tag{5}$$

$$B_{\alpha\beta} = \int_{-h}^{\eta} \frac{\partial Z_\alpha}{\partial z}\frac{\partial Z_\beta}{\partial z}\, dz \tag{6}$$

$$C_{\alpha\beta} = \int_{-h}^{\eta} \frac{\partial Z_\alpha}{\partial h} Z_\beta\, dz \tag{7}$$

Unknown functions in Eqs. (2) and (3) are f_α ($\alpha = 1$ to N) and η which yield $N+1$ unknowns, whereas the total number of equations is also $N+1$. No assumptions other than expanding the velocity potential into a series are made in deriving the equations. Therefore, the nonlinear mild-slope equations can be used to simulate even strongly nonlinear and strongly dispersive wave transformation.

2.2 Vertical distribution functions

Since the present study deals with wave transformation in shallow water, even-order polynomial functions are chosen as vertical distribution functions:

$$Z_\alpha = \left(\frac{h+z}{h}\right)^{2(\alpha-1)} \tag{8}$$

Then, Eqs. (4) to (7) become

$$Z_\alpha^\eta = \zeta^{2(\alpha-1)} \tag{9}$$

$$A_{\alpha\beta} = h\frac{\zeta^{2(\alpha+\beta)-3}}{2(\alpha+\beta)-3} \tag{10}$$

$$B_{\alpha\beta} = \frac{4(\alpha-1)(\beta-1)}{h}\frac{\zeta^{2(\alpha+\beta)-5}}{2(\alpha+\beta)-5} \tag{11}$$

$$C_{\alpha\beta} = 2(\alpha - 1)\left[\frac{\zeta^{2(\alpha+\beta)-4}}{2(\alpha+\beta)-4} - \frac{\zeta^{2(\alpha+\beta)-3}}{2(\alpha+\beta)-3}\right] \tag{12}$$

where

$$\zeta = \frac{h+\eta}{h} \tag{13}$$

In the following calculation, the series is trancated at the second term (N=2) as

$$\phi(x,y,z) = f_1(x,y,t) + \left(1 + \frac{z}{h}\right)^2 f_2(x,y,t) \tag{14}$$

so that Eqs. (2) and (3) are rewritten in more specific forms:

$$g\eta + \frac{\partial f_1}{\partial t} + \frac{(h+\eta)^2}{h^2}\frac{\partial f_2}{\partial t} + \frac{1}{2}\left[\nabla f_1 + \frac{(h+\eta)^2}{h^2}\nabla f_2\right]^2 + \frac{1}{2}\left[\frac{2(h+\eta)}{h^2}f_2\right]^2$$
$$-\frac{2\eta(h+\eta)}{h^3}f_2\left[\nabla f_1 + \frac{(h+\eta)^2}{h^2}\nabla f_2\right]\nabla h = 0 \tag{15}$$

$$\frac{\partial \eta}{\partial t} + \nabla\left[(h+\eta)\nabla f_1 + \frac{(h+\eta)^3}{3h^2}\nabla f_2\right] + \frac{(h+\eta)^2(h-2\eta)}{3h^3}\nabla f_2 \nabla h$$
$$-\frac{2(h+\eta)\eta}{h^3}f_2\nabla\eta\nabla h = 0 \tag{16}$$

$$\frac{(h+\eta)^2}{h^2}\frac{\partial \eta}{\partial t} + \nabla\left[\frac{(h+\eta)^3}{3h^2}\nabla f_1 + \frac{(h+\eta)^5}{5h^4}\nabla f_2\right] - \frac{4(h+\eta)^3}{3h^4}f_2$$
$$-\frac{(h+\eta)^2(h-2\eta)}{3h^3}\nabla f_1 \nabla h - \frac{2(h+\eta)^3}{h^5}f_2\nabla\eta\nabla h = 0 \tag{17}$$

2.3 Boundary condition

We first consider one-dimensional (on-offshore) wave transformation. At the onshore boundary, waves propagate only shoreward (i.e., positive x direction) with wave celerity, C so that for any independent variable, Φ ($= \eta$, f_1 or f_2),

$$\Phi = \Phi(x - Ct) \tag{18}$$

At the offshore boundary, waves consist of incident and reflected waves denoted by $\Phi_{\rm in}$ and $\Phi_{\rm r}$, respectively:

$$\Phi = \Phi_{\rm in}(x - Ct) + \Phi_{\rm r}(x + Ct) \tag{19}$$

where the incident waves are given and the reflected waves are unknown.

Differentiating the above two equations with respect to x and t, we obtain the following boundary conditions:

$$\frac{\partial \Phi}{\partial t} + C\frac{\partial \Phi}{\partial x} = 0 \quad \text{(at onshore boundary)} \tag{20}$$

$$\frac{\partial \Phi}{\partial t} - C\frac{\partial \Phi}{\partial x} - 2\frac{\partial \Phi_{\rm in}}{\partial t} = 0 \quad \text{(at offshore boundary)} \tag{21}$$

The water surface elevation, η_{in}, due to the incident waves can be given from an appropriate progressive wave theory from given water depth h, wave period T, and wave height H. The functions, $f_{1\text{in}}$ and $f_{2\text{in}}$, should also be able to be given from the same wave theory, but an explicit expression is not available in any wave theory. However, since nonlinearity is normally negligible at the offshore boundary, linear relationships between η_{in}, and $f_{1\text{in}}$ and $f_{2\text{in}}$ are derived as follows.

One-dimensional linerized forms of Eqs. (15) to (17) for a constant depth are written as follows:

$$g\eta + \frac{\partial f_1}{\partial t} + \frac{\partial f_2}{\partial t} = 0 \tag{22}$$

$$\frac{\partial \eta}{\partial t} + h\frac{\partial^2 f_1}{\partial x^2} + \frac{h}{3}\frac{\partial^2 f_2}{\partial x^2} = 0 \tag{23}$$

$$\frac{\partial \eta}{\partial t} + \frac{h}{3}\frac{\partial^2 f_1}{\partial x^2} + \frac{h}{5}\frac{\partial^2 f_2}{\partial x^2} - \frac{4}{3h}f_2 = 0 \tag{24}$$

which result in an eigenvalue problem for η, f_1 and f_2. To solve the problem, we seek for a non-trivial solution of the following forms:

$$\eta = ae^{i(kx-\omega t)} \tag{25}$$

$$f_1 = a_1 e^{i(kx-\omega t)} \tag{26}$$

$$f_2 = a_2 e^{i(kx-\omega t)} \tag{27}$$

where ω $(= 2\pi/T)$ is the angular frequency to be given, k the wave number to be determined from the eigen value, and a, a_1 and a_2 are the amplitudes.

By differentiating Eq. (22) with respect to t and substituting it into Eqs. (23) and (24), η can be eliminated:

$$-\frac{1}{g}\left(\frac{\partial^2 f_1}{\partial t^2} + \frac{\partial^2 f_2}{\partial t^2}\right) + h\frac{\partial^2 f_1}{\partial x^2} + \frac{h}{3}\frac{\partial^2 f_2}{\partial x^2} = 0 \tag{28}$$

$$-\frac{1}{g}\left(\frac{\partial^2 f_1}{\partial t^2} + \frac{\partial^2 f_2}{\partial t^2}\right) + \frac{h}{3}\frac{\partial^2 f_1}{\partial x^2} + \frac{h}{5}\frac{\partial^2 f_2}{\partial x^2} - \frac{4}{3h}f_2 = 0 \tag{29}$$

Then substitution of Eqs. (26) and (27) into the above two equations yield the following two equations:

$$\frac{\omega^2}{g}(a_1 + a_2) - hk^2 a_1 - \frac{hk^2}{3}a_2 = 0 \tag{30}$$

$$\frac{\omega^2}{g}(a_1 + a_2) - \frac{hk^2}{3}a_1 - \frac{hk^2}{5}a_2 - \frac{4}{3h}a_2 = 0 \tag{31}$$

To obtain a non-trivial solution, the determinant of the above simultaneous equations should vanish, from which we can determine the wave number as

$$k^2 = \frac{6h^2\omega^2 - 15gh \pm \sqrt{(6h^2\omega^2 - 15gh)^2 + 60gh^3\omega^2}}{2gh^3} \tag{32}$$

in which positive sign should be selected because positive and negative signs, respectively, yield positive and negative values of k^2 corresponding to progressive and evernecsent waves. Then the normalized eigenvector, (r_1, r_2), becomes

$$r_1 = \frac{a_1}{a_1 + a_2} = \frac{3\omega^2}{2ghk^2} - \frac{1}{2} \tag{33}$$

$$r_2 = \frac{a_2}{a_1 + a_2} = \frac{3}{2} - \frac{3\omega^2}{2ghk^2} \tag{34}$$

By considering Eqs. (22), (25) to (27), (33) and (34), we finally obtain the following relationships:

$$f_{1\text{in}} = \frac{g}{i\omega}\left(\frac{3\omega^2}{2ghk^2} - \frac{1}{2}\right)\eta_{\text{in}} \tag{35}$$

$$f_{2\text{in}} = \frac{g}{i\omega}\left(\frac{3}{2} - \frac{3\omega^2}{2ghk^2}\right)\eta_{\text{in}} \tag{36}$$

The above relationships will be used even when a nonlinear wave theory such as Stokes or cnoidal wave theory is employed to give incident waves because nonlinearity is normally not so strong at the offshore boundary.

3 Computational Method and Condition

Eqs. (15) to (17) are solved numerically by an implict finite difference scheme. The initial condition is still water and the time evolution of η, f_1 and f_2 is calculated by these equations as well as the boundary conditions (20) and (21). Spatial derivatives are evaluated at the center of the old and new time steps. This necessitates an iteration procedure, for which the Newton-Raphson method is employed in the present study.

The computational domain is 500m long including a submerged breakwater or a step. The grid size is 1/64 of the wavelegth, and the time increment is 1/64 of the wave period. This fine grid size assures the accuracy of the numerical solution for the nonlinear mild-slope equations.

To give incident waves, a third-order Stokes wave theory and a second-order cnoidal wave theory (Isobe and Kraus, 1983a, b) are employed depending on the Ursell parameter. Stokes wave theory is employed when the Ursell parameter is less than 25, and cnoidal wave theory is employed otherwise.

The incident wave conditions for close examination of the numerical result are shown in **Table 1**.

Table 1 Incident wave condition for numerical experiment

	wave period (s)	wave height (m)	water depth (m)
Case 1	7.1	1.0	10.0
Case 2	7.1	2.0	10.0

Two types of bottom configuration are employed: step type and submerged breakwater type. Samples are shown in **Figure 1** and detailed dimensions used are shown in **Table 2**.

Table 2 Bottom configuration

step		
slope of step	$\tan\theta$	1/3, 1/5, 1/10, 1/20
relative depth on step	h_s/h	0.2, 0.3, 0.4, 0.5, 0.6, 0.7

submerged breakwater		
relative crown depth	h_s/h	0.2, 0.3, 0.4, 0.5, 0.6, 0.7
relative crown width	b/h	2, 4, 6, 8, 10, 12, 14, 16, 20, 22

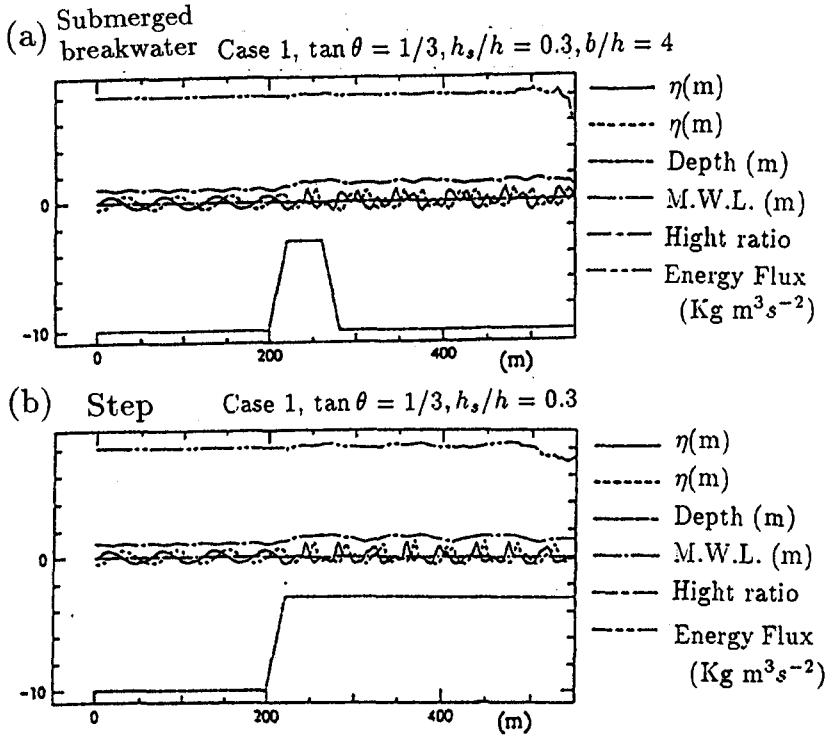

Figure 1 Examles of calculated distribution of the water surface elevation, wave height, mean water level, and energy flux.

4 Result for 1-D Calculation

Figure 1 shows examples of calculated distribution of the water surface elevation at two different time steps, wave height, mean water level, and energy flux. Waves are incident from left to right. **(a)** is for a submerged breakwater, and **(b)** is for a step. The energy flux is kept constant except for a small fluctuation which may have resulted from the error due to insufficient number of terms in the series expansion of the velocity potential. As can be seen from the water surface elevation, wave disintegration on the breakwater or step is significant.

To examine the nonlinear wave disintegration, the temporal change of water surface elevation is transformed into a Fourier series at every point. **Figure 2** shows the distribution of amplitude of the first six components. Spatial change of amplitudes on the step are periodic.

The spacing between two adjacent peaks of the second harmonics is derived theoret-

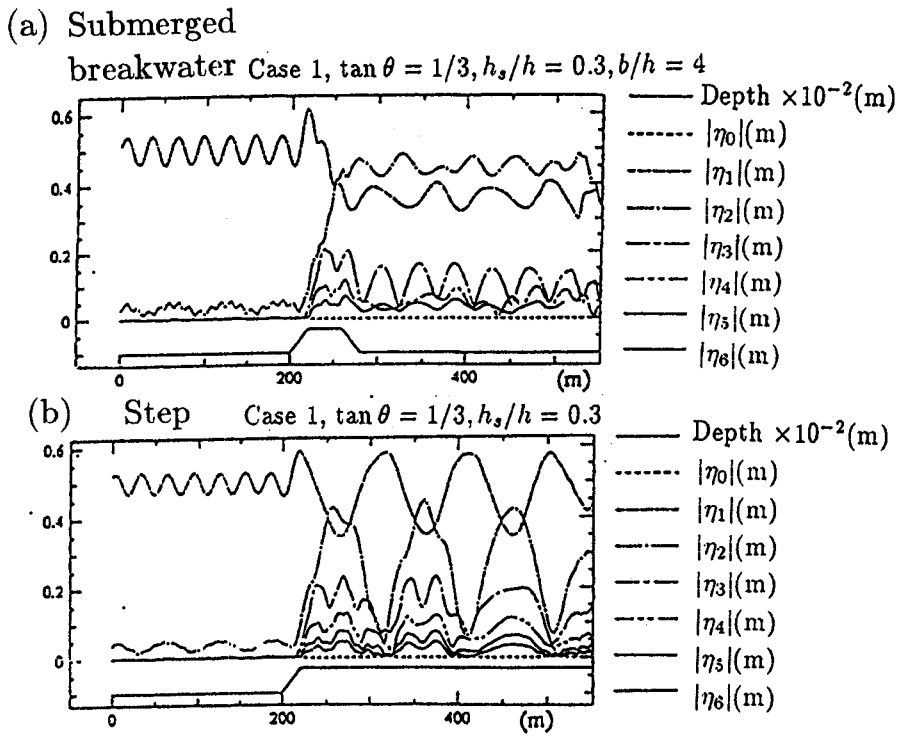

Figure 2 Distribution of amplitude of various harmonics.

ically as (Massel, 1983)

$$\lambda_2 = 2\pi/(k_2 - 2k_1) \tag{37}$$

where k_1 and k_2 are the wave numbers corresponding to the linear dispersion relation for ω and 2ω, respectively:

$$\omega^2 = gk_1 \tanh k_1 h \tag{38}$$

$$4\omega^2 = gk_2 \tanh k_2 h \tag{39}$$

The present result agrees well with the above theory, which implies the return spacing is predicted theoretically. However, the amplitude cannot be predicted accurately expecially for strongly nonlinear cases. Thus, it is examined in the present study in detail.

Figure 3 shows the relation between the maximum amplitudes, $|\eta_n|$ ($n = 1$ to 3), of the first three harmonics, and the slope, $\tan\theta$, of the offshoreward face of a step. The maximum amplitude of higher harmonics increases with increasing slope. The effect of the water depth on a step is shown in **Figure 4**. In the figure, h_s/h is the ratio between the water depth, h_s, on the step and that, h, in the offshore region. Results are plotted for non-breaking cases for which $h_s/h \geq 0.3$ for Case 1 and $h_s/h \geq 0.5$ for Case 2. The maximum amplitudes of higher harmonics increase with decreasing water depth on the step.

As can be expected from the periodicity of the amplitude of higher harmonics on the step which is shown in **Figure 2(b)**, the amplitudes of various harmonics behind a submerged breakwater oscillate significantly with the width. **Figure 5** shows the average amplitudes of the first three harmonics behind a submerged breakwater. **(a)** is for the incident waves of Case 1 and $h_s/h = 0.3$, **(b)** for Case 1 and $h_s/h = 0.5$, and **(c)** for Case 2 and $h_s/h = 0.5$. For each figure, the return spacing, λ_2, of the second harmonics agrees well with that predicted by Eq. (37). The amplitude behind the breakwater becomes maximum for $b = m\lambda_2$ ($m = 1, 2, \cdots$), and minimum for $b = (m - 1/2)\lambda_2$, and the difference between the maximum and minimum values increases with

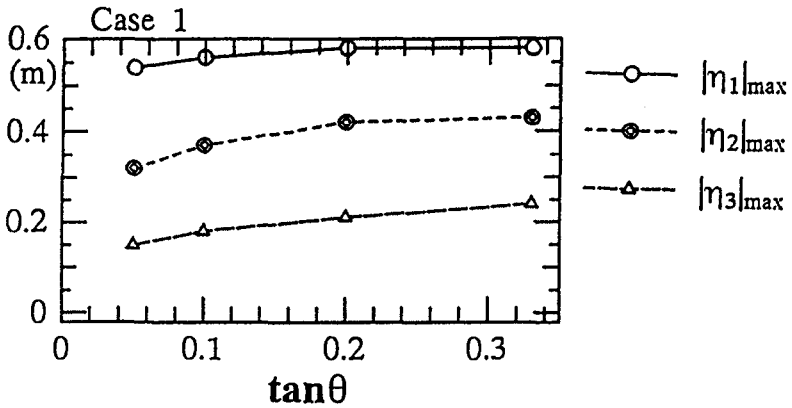

Figure 3 Relation between the maximum amplitude of various harmonics and the slope of the offshoreward face of a step.

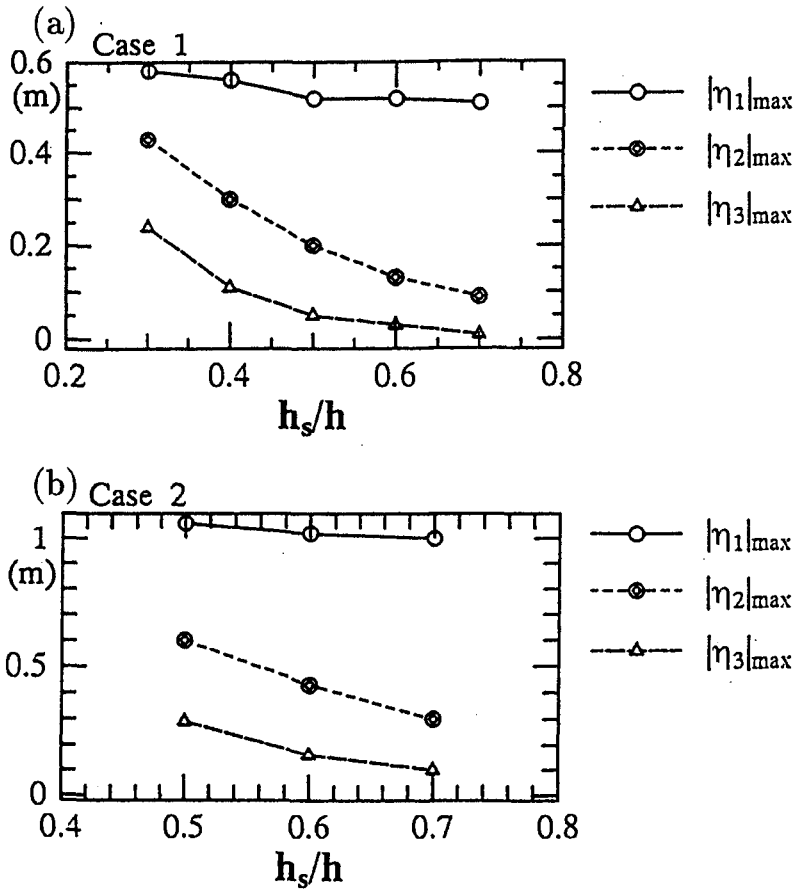

Figure 4 Relation between the maximum amplitude of various harmonics and the water depth on a step.

decreasing crown water depth. By comparing between (**b**) and (**c**), it is understood that the ratios of amplitudes of higher harmonics to the first harmonics grow larger for larger incident wave steepness.

The above results imply that significant amount of wave energy is transferred from the fundamental component to higher harmonics and the amplitude of the second harmonics can become comparable or larger than that of the first harmonics behind a submerged breakwater by adjusting its configuration.

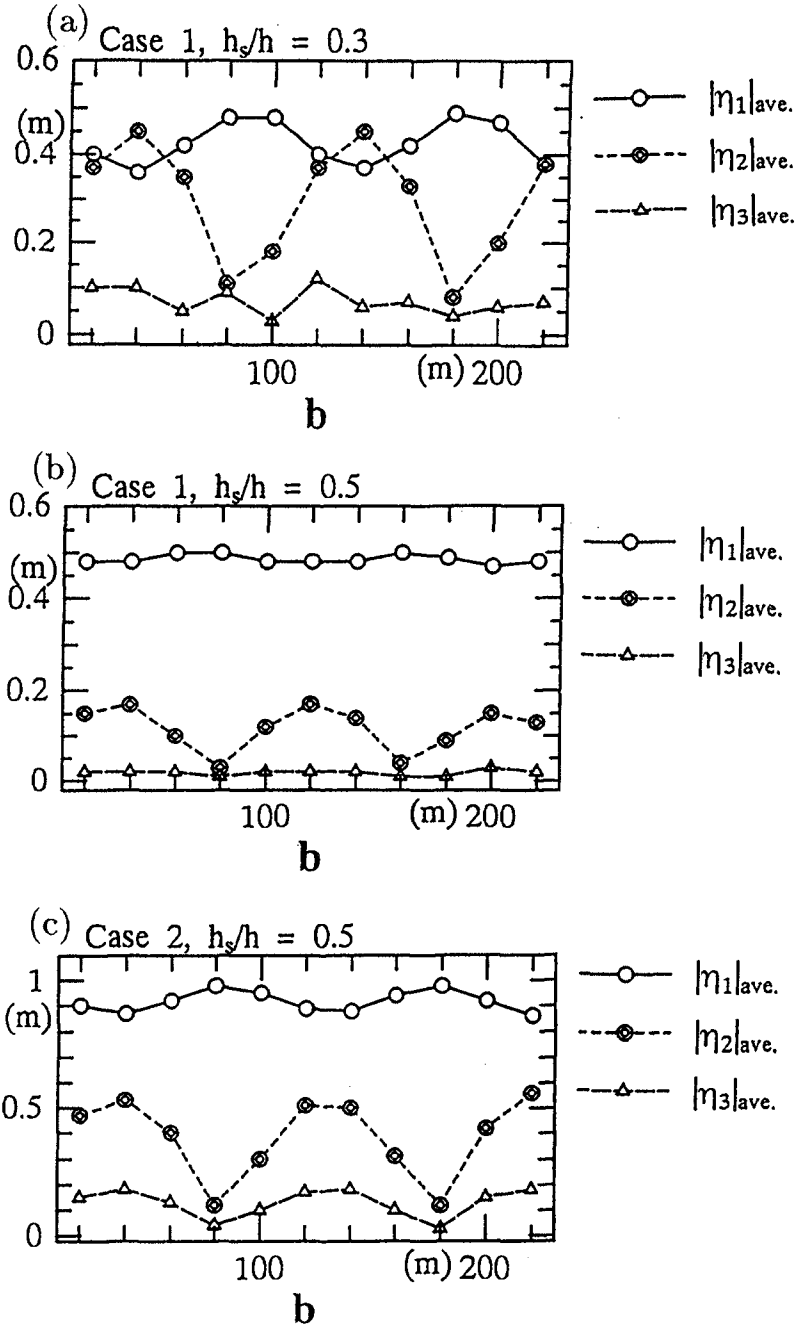

Figure 5 Relation between the average amplitude of various harmonics and the crown width of a submerged breakwater.

5 Basic Equations for Obliquely-Incident Waves

When waves are incident obliquely to a region with parallel depth contours, the celerity, C_y, in the alongshore direction, y, becomes constant throughout the depth. The quantity C_y is evaluated at the offshore boundary as

$$C_y = \frac{C_o}{\sin\theta_o} \tag{40}$$

where C_o and θ_o are the wave celerity and direction at the offshore boundary. Then the derivative with respect to y is converted to that with respect to t:

$$\frac{\partial}{\partial y} = \frac{1}{C_y}\frac{\partial}{\partial t} \tag{41}$$

If Eq. (41) is substituted into Eqs. (15) to (17), independent variables become only x and t. However, numerical solution could not be obtained due to numerical instability because the equations include the second-order derivatives with respect to t. Therefore, by considering the linear relationships (35) and (36), the following equations are used to eliminate the second-order derivatives:

$$\frac{\partial^2 f_1}{\partial t^2} = -gr_1\frac{\partial\eta}{\partial t} \tag{42}$$

$$\frac{\partial^2 f_2}{\partial t^2} = -gr_2\frac{\partial\eta}{\partial t} \tag{43}$$

Then Eqs. (15) to (17) become

$$g\eta + \frac{\partial f_1}{\partial t} + \frac{(h+\eta)^2}{h^2}\frac{\partial f_2}{\partial t} + \frac{1}{2}\left[\frac{\partial f_1}{\partial x} + \frac{(h+\eta)^2}{h^2}\frac{\partial f_2}{\partial x}\right]^2 + \frac{1}{2}\frac{1}{C_y^2}\left[\frac{\partial f_1}{\partial t} + \frac{(h+\eta)^2}{h^2}\frac{\partial f_2}{\partial t}\right]^2$$
$$+\frac{1}{2}\left[\frac{2(h+\eta)}{h^2}f_2\right]^2 - \frac{2\eta(h+\eta)}{h^3}f_2\left[\frac{\partial f_1}{\partial x} + \frac{(h+\eta)^2}{h^2}\frac{\partial f_2}{\partial x}\right]\frac{\partial h}{\partial x} = 0 \tag{44}$$

$$\frac{\partial\eta}{\partial t} + \frac{\partial}{\partial x}\left[(h+\eta)\frac{\partial f_1}{\partial x} + \frac{(h+\eta)^3}{3h^2}\frac{\partial f_2}{\partial x}\right]$$
$$+\frac{1}{C_y^2}\left[\left\{\frac{\partial f_1}{\partial t} + \frac{(h+\eta)^2}{h^2}\frac{\partial f_2}{\partial t} - gr_1(h+\eta) - gr_2\frac{(h+\eta)^3}{3h^2}\right\}\frac{\partial\eta}{\partial t}\right]$$
$$+\frac{(h+\eta)^2(h-2\eta)}{3h^3}\frac{\partial f_2}{\partial x}\frac{\partial h}{\partial x} - \frac{2(h+\eta)\eta}{h^3}f_2\frac{\partial\eta}{\partial x}\frac{\partial h}{\partial x} = 0 \tag{45}$$

$$\frac{(h+\eta)^2}{h^2}\frac{\partial\eta}{\partial t} + \frac{\partial}{\partial x}\left[\frac{(h+\eta)^3}{3h^2}\frac{\partial f_1}{\partial x} + \frac{(h+\eta)^5}{5h^4}\frac{\partial f_2}{\partial x}\right]$$
$$+\frac{1}{C_y^2}\left[\left\{\frac{(h+\eta)^2}{h^2}\frac{\partial f_1}{\partial t} + \frac{(h+\eta)^4}{h^4}\frac{\partial f_2}{\partial t} - gr_1\frac{(h+\eta)^3}{3h^2} - gr_2\frac{(h+\eta)^5}{5h^4}\right\}\frac{\partial\eta}{\partial t}\right]$$
$$-\frac{4(h+\eta)^3}{3h^4}f_2 - \frac{(h+\eta)^2(h-2\eta)}{3h^3}\frac{\partial f_1}{\partial x}\frac{\partial h}{\partial x} - \frac{2(h+\eta)^3\eta}{h^5}f_2\frac{\partial\eta}{\partial x}\frac{\partial h}{\partial x} = 0 \tag{46}$$

The numerical solution method for the above equations is the same as that for normal incidence previously described.

6 Result for Obliquely-Incident Waves

Once a numerical solution is obtained in terms of x and t as $\Phi(x,t)$, the solution in terms of x, y and t is written as $\Phi(x, t - y/C_y)$. **Figure 6** shows the pattern of wave crests near an infinitively-long submerged breakwater with a trapezoidal cross section. Waves are incident obliquely from the lower boundary.

For **Figure 6(a)**, wave direction changes on the breakwater due to refraction, and secondary crests appear due to the nonlinear effect, but the secondary crests disappear behind the breakwater and the wave direction turns back to that of the incident waves. However, for **Figure 6(b)** in which the amplitude of the second harmonics grows larger than that of the first harmonics, secondary crests remain behind the breakwater and the wave direction is different from that of incident waves. The reason is as follows. Since celerities of all component waves must be the same in the y direction, higher harmonics, of which the wave celerities are smaller than that of fundamental component, should propagate in the direction closer to the shore-normal. Therefore, the predominant direction changes when higher harmonic components dominate behind the breakwater.

7 Conclusion

Numerical scheme for the nonlinear mild-slope equations is developed to examine wave transformation due to a submerged breakwater for normal and oblique incidence.

Generation of higher harmonics for normal incidence to a step and a submerged breakwater is first examined. The amplitudes of higher harmonics on a submerged breakwater are larger for steeper offshoreward slope and for smaller crown water depth. The amplitudes of higher harmonics behind a submerged breakwater become maximum for $b = m\lambda_2$ $(m = 1, 2, \cdots)$, and minimum for $b = (m - 1/2)\lambda_2$. When the nonlinearity of incident waves is stronger, higher harmonics grow larger.

Higer harmonics appear also for obliquely incident waves. When higher harmonics dominate behind the submerged breakwater, predominant wave direction chnges to keep the alongshore celerity constant.

These results imply that, utilizing a submerged breakwater, we can control wave period and direction as well as wave height.

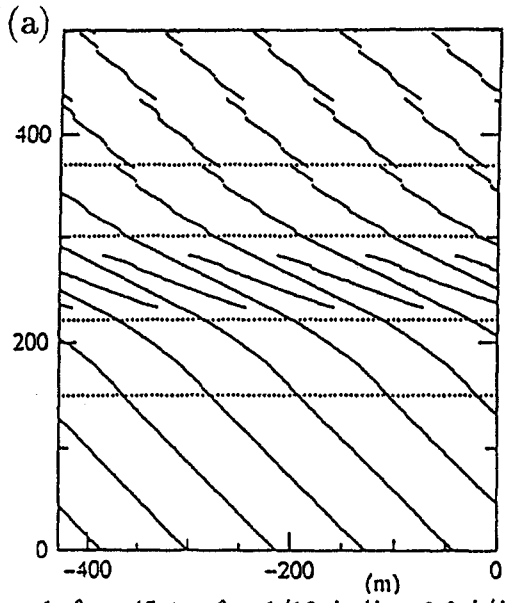

Case 1, $\theta_0 = 45, \tan\theta = 1/10, h_s/h = 0.3, b/h = 8$

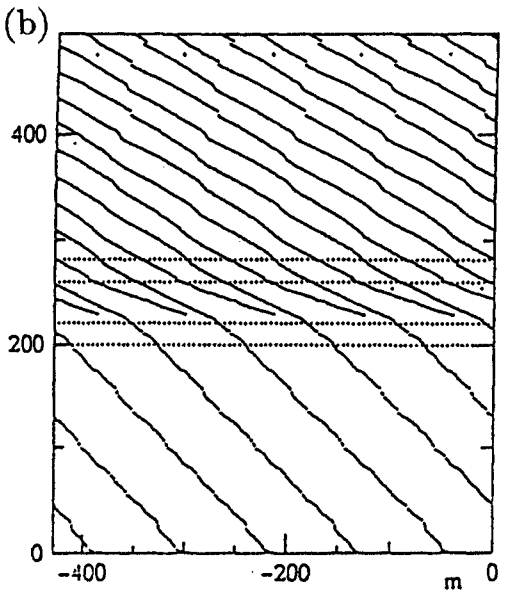

Case 1, $\theta_0 = 45, \tan\theta = 1/3, h_s/h = 0.3, b/h = 4$

Figure 6 Change of crest lines due to a submerged breakwater.

References

[1] Isobe, M. (1994): Time-dependent mild-slope equations for random waves, Proc. 24th Int. Conf. on Coastal Eng., ASCE, pp. 285–299.

[2] Isobe, M. and N. C. Kraus (1983): Derivation of a third-order Stokes wave theory, Hydraulics Lab. Rep., Dept. of Civil Eng., Yokohama Nat. Univ., No. YNU-HY-83-1, 32p.

[3] Isobe, M. and N. C. Kraus (1983): Derivation of a second-order cnoidal wave theory, Hydraulics Lab. Rep., Dept. of Civil Eng., Yokohama Nat. Univ., No. YNU-HY-83-2, 43p.

[4] Luke, J. C. (1967): A variational principle for a fluid with a free surface, J. Fluid Mech., Vol. 27, pp. 395–397.

[5] Massel, S. R. (1983): Harmonic generation by waves propagating over a submerged step, Coastal Eng., Vol. 7, pp. 357–380.

[6] Nadaoka, K., S. Beji and Y. Nakagawa (1994): A fully-dispersive nonlinear wave model and its numerical solution, Proc. 24th Int. Conf. on Coastal Eng., ASCE, pp. 427–441.

[7] Nochino, M. (1994): Fully-nonlinear coupled vibration equations for irregular water waves and their basic characteristics, Proc. 41st Japanese Conf. on Coastal Eng., JSCE, pp. 16–20(inJapanese).

[8] Ohyama, T. and K. Nadaoka (1992): Modeling the transformation of nonlinear waves passing over a submerged dike, Proc. 23rd Int. Conf. on Coastal Eng., ASCE, pp. 526–539.

[9] Ohyama, T. and K. Nadaoka (1994): Transformation of a nonlinear wave train passing over a submerged shelf without breaking, Coastal Eng., Vol. 24, No. 1-2, pp. 1–22.

[10] Tsubota, H., M. Isobe and A. Watanabe (1994): Study on wave control by submerged breakwater, Proc. Coastal Eng., JSCE, Vol. 41, pp. 641–645.